

Published in final edited form as:

Nature. 2008 November 13; 456(7219): 259–263. doi:10.1038/nature07416.

A unique role for autophagy and *Atg16L1* in Paneth cells in murine and human intestine

Ken Cadwell¹, John Liu¹, Sarah L. Brown¹, Hiroyuki Miyoshi¹, Joy Loh¹, Jochen Lennerz¹, Chieko Kishi², Wumesh KC¹, Javier A. Carrero¹, Steven Hunt³, Christian Stone⁴, Elizabeth M. Brunt¹, Ramnik J. Xavier⁵, Barry P. Sleckman¹, Ellen Li⁴, Noboru Mizushima², Thaddeus S. Stappenbeck^{1,*†}, and Herbert W. Virgin IV^{1,6,*†}

¹Department of Pathology and Immunology, Washington University School of Medicine, St. Louis, MO 63110, USA

²Department of Physiology and Cell Biology, Tokyo Medical and Dental University Graduate School and Faculty of Medicine, Tokyo, Japan, 113–8519

³Department of Surgery, Washington University School of Medicine, St. Louis, MO 63110, USA

⁴Department of Medicine, Washington University School of Medicine, St. Louis, MO 63110, USA

⁵Center for Computational and Integrative Biology and Gastrointestinal Unit, Massachusetts General Hospital, Harvard Medical School, Boston, MA 02114, USA

⁶Department of Molecular Microbiology, Washington University School of Medicine, St. Louis, MO 63110, USA.

Abstract

Susceptibility to Crohn's disease (CD), a complex inflammatory disease involving the small intestine, is controlled by up to 32 loci¹. One CD risk allele is in *ATG16L1*, a gene homologous to the essential yeast autophagy gene *ATG16*². It is not known how Atg16L1 or autophagy contributes to intestinal biology or CD pathogenesis. To address these questions we generated and characterized mice that are hypomorphic for Atg16L1 protein expression, and validated conclusions based on studies in these mice by analyzing intestinal tissues that we collected from CD patients carrying the CD risk allele of *ATG16L1*. We show that Atg16L1 is a *bona fide* autophagy protein. Within the ileal epithelium, both Atg16L1 and a second essential autophagy protein Atg5 are selectively important for the biology of the Paneth cell, a specialized epithelial cell which functions in part by secretion of granule contents containing antimicrobial peptides and other proteins that alter the intestinal environment³. Atg16L1 and Atg5-deficient Paneth cells exhibited striking abnormalities in the granule exocytosis pathway. In addition, transcriptional analysis revealed an unexpected gain of function specific to Atg16L1-

*To whom correspondence should be addressed: Dr. Herbert W. Virgin IV, Department of Pathology and Immunology, Washington University School of Medicine, 660 S. Euclid Ave, Box 8118, St. Louis, MO 63110. Telephone: (314) 362–9223. Fax: (314) 362–4096. Email: E-mail: virgin@wustl.edu. Dr. Thaddeus S. Stappenbeck, Department of Pathology and Immunology, Washington University School of Medicine, 660 S. Euclid Ave, Box 8118, St. Louis, MO 63110. Telephone: (314) 362–4214. Fax: (314) 362–7487. Email: E-mail: stappenb@wustl.edu.. **Author Information** The authors declare no competing financial interests. Correspondence and requests for materials should be addressed to H.W.V. (E-mail: virgin@wustl.edu) and T.S.S. (E-mail: stappenb@wustl.edu)..

[†]These authors contributed equally to this work.

Author Contributions The original hypothesis of the article was formulated by K.C., H.W.V., and T.S.S. Autophagy experiments were performed by K.C. and C.K. Mouse lines were established by K.C., J.Loh, and B.P.S. Mouse analysis experiments were performed by K.C., J.Liu, S.L.B., H.M., W.K., T.S.S., and J.Lennerz. Histological examination was performed by T.S.S., E.M.B., and J.Lennerz. *L. monocytogenes* experiments were performed by J.C. and K.C. Microarray analysis was performed by R.J.X. and T.S.S. Human tissue collection, genotyping, and preparation were performed by E.L., S.H., and C.S. N.M. provided advice, antibody to Atg16L1, and experiments by C.K. were performed in his lab. The manuscript was written by K.C., H.W.V., and T.S.S. and all authors commented on the manuscript, data, and conclusions prior to submission.

Supplementary Information accompanies the paper on www.nature.com/nature.

deficient Paneth cells including increased expression of genes involved in PPAR signaling and lipid metabolism, acute phase reactants, as well as two adipocytokines, leptin and adiponectin, known to directly influence intestinal injury responses. Importantly, CD patients homozygous for the *ATG16L1* CD risk allele displayed Paneth cell granule abnormalities similar to those observed in autophagy protein-deficient mice and expressed increased levels of leptin protein. Thus, Atg16L1, and likely the process of autophagy, play their role within the intestinal epithelium of mice and CD patients by selective effects on the cell biology and specialized regulatory properties of Paneth cells.

Crohn's disease typically involves the distal ileum and in its most severe form is characterized by pathological changes including transmural acute and chronic inflammation. CD is associated with increased expression of immunoregulatory cytokines including leptin⁴ and adiponectin⁵. Multiple genetic factors predispose to CD, but the specific relationship between the function of these genes and the diverse pathologies observed in CD is not well understood. One CD susceptibility allele is in the predicted autophagy gene *ATG16L1*^{6,7,8,9}. Autophagy is an evolutionarily conserved process that recycles cellular components via delivery of double membrane-bound vesicles containing cytoplasm and cytoplasmic organelles to the lysosome¹⁰. Autophagy has an important role in cell and tissue homeostasis, and has been implicated in a range of human diseases¹⁰. The mammalian Atg16L1 protein contains an N-terminal domain that is homologous to yeast Atg16² which functions in autophagy as part of a complex with autophagy proteins Atg5 and Atg12^{2,11}. Atg16 is responsible, in both yeast and mammalian cells, for proper sub-cellular localization of the autophagy machinery^{12,8,11}.

To determine the role of Atg16L1 and autophagy in the intestine, we generated two mouse lines with gene trap-mediated disruptions of *Atg16L1* and a third line lacking *Atg5* in intestinal epithelial cells. Gene trap vectors introduce a false splice acceptor into an intron, and can inhibit expression of intact mRNA¹³ (Fig. 1a). This can result in decreased expression of a protein, potentially generating viable mice when full disruption of a gene is lethal. This approach is attractive since Atg5 is part of the Atg16L1 complex and full disruption of *Atg5* is lethal^{14,2}. Mouse lines homozygous for gene trap mutations were generated from commercially available ES cells carrying gene trap mutations in the intron 3' to either exon 6 or exon 10 of *Atg16L1*¹³. *Atg16L1* mutant murine embryo fibroblasts (MEFs) expressed low levels of Atg16L1 protein (Fig. 1b) indicating that both mouse lines, Atg16L1^{HM1} and Atg16L1^{HM2}, are hypomorphic (HM) for expression of Atg16L1 protein. Atg16L1^{HM} mice were born at Mendelian ratios (Supplementary Fig. 1a), and survive to adulthood; the characteristics of the two Atg16L1^{HM} lines *in vivo* were similar across all experiments.

To determine if Atg16L1 is an autophagy protein, we studied low-passage and transformed MEFs from Atg16L1^{HM} mice compared to MEFs lacking the essential autophagy protein Atg5¹⁴. Rapamycin-induced and autophagy-dependent¹⁵ degradation of the adapter protein p62 was diminished in Atg16L1^{HM} and Atg5^{-/-} cells (Fig. 1c-e). Decreased degradation of p62 in Atg16L1^{HM} cells was restored by expressing Atg16L1 (Supplementary Fig. 1b, c). Atg16L1^{HM} MEFs also showed diminished rapamycin-induced production of LC3-II, the phosphatidylethanolamine-conjugated form of Atg8/LC3-I generated during autophagy¹⁰ (Fig. 1e, f). The induction of autophagosomes, as measured by LC3-positive dot formation after rapamycin treatment or starvation, was also decreased in Atg16L1^{HM} MEFs (Supplementary Fig. 2), although the defect of Atg16L1^{HM2} cells was more subtle in starved cells; this was confirmed in cells transfected with GFP-LC3 (Supplementary Fig. 3). Mammalian Atg16L1 is therefore an autophagy protein.

We next determined if markers of autophagy were abnormal in the distal small intestine (ileum, a common site of CD) of Atg16L1^{HM} mice by measuring the expression of Atg16L1, LC3, and p62 proteins in ileal lysates (Fig. 1g-i). Atg16L1 mRNA is expressed throughout the crypt-

villus axis (Supplementary Fig. 4). Atg16L1^{HM} mice expressed 23–37% of the expected level of Atg16L1 protein (Fig. 1g, h). Consistent with a role for Atg16L1 in ileal autophagy, both the ratio of LC3-I to LC3-II, and the total amount of LC3-I and p62 were increased in lysates from Atg16L1^{HM} mice (Fig. 1g, i). To validate these results, we studied ileal lysates from mice generated by breeding *Atg5^{flox/flox}* mice¹⁶ to mice expressing the Cre recombinase under the control of the intestinal epithelium-specific *villin* promoter (*Atg5^{flox/flox}villin-Cre* mice)¹⁷. Atg5 expression was significantly diminished in ileal lysates of *Atg5^{flox/flox}villin-Cre* mice, and these mice exhibited changes in expression of LC3 and p62 similar to those observed in Atg16L1^{HM} mice (Supplementary Fig. 5). These data are consistent with a role for Atg16L1 and Atg5 in ileal autophagy.

Deficiency in Atg16L1 had no effect on the overall morphology of the ileum or colon as measured by analysis of crypt height or villus length (data not shown). However, there were obvious abnormalities in Paneth cells, leading us to focus our studies on these critically important intestinal innate immune cells. Paneth cells are ileal epithelial cells thought to play a role in control of intestinal microbiota via secretion of granule contents including antimicrobial peptides and lysozyme¹⁸. Staining of whole mounts of ileum revealed the expected colocalization of lysozyme and mucus (Fig. 2a). However, there was a striking lack of lysozyme staining in the mucus of Atg16L1^{HM} mice, suggesting an abnormality of Paneth cell secretion (Fig. 2b). We examined PAS/alcian blue stained sections and found extraordinary abnormalities in Paneth cells including aberrant, disorganized granules as well as decreased granule numbers (Fig 2c, d, and not shown). Blinded analysis of these sections from 16 control and 30 mutant mice revealed a 100% concordance between Atg16L1^{HM} genotype and abnormal Paneth cell morphology. We quantified these Paneth granule abnormalities by staining sections for lysozyme which is normally packaged efficiently in the granules¹⁸ (Fig. 2e-h). In these sections, we observed a striking population of Atg16L1^{HM} cells with diffuse lysozyme staining (Fig. 2f, h). We also observed the presence of intact granules in the crypt lumen of whole mounts of ileum from Atg16L1^{HM} mice (Supplementary Fig. 6a-c), a finding confirmed by EM (Supplementary Figure 6d, e), potentially explaining the absence of lysozyme staining in the mucus layer of the ileum (Fig. 3a, b). These observations indicate that Atg16L1 is required for maintaining the integrity of the Paneth cell granule exocytosis pathway. Based on these data, and the published role for Nod2 in resistance to infection¹⁹, we orally challenged Atg16L1^{HM} mice with *Listeria monocytogenes*. We found no change in *L. monocytogenes* titers in spleen, liver, and mesenteric lymph nodes (Supplementary Fig. 7), indicating that the striking changes in release of granules in ATG16L1^{HM} mice did not affect *L. monocytogenes* resistance. This argues that the phenotypes of mutations analyzed to date in Atg16L1 and Nod 2 are distinct.

Despite these profound alterations in the granule exocytosis pathway, we found no evidence of increased epithelial cell death or proliferation as determined by quantification of apoptotic bodies and M-phase cells (not shown). Importantly, deletion of *Atg5* in the intestinal epithelium in *Atg5^{flox/flox}villin-Cre* mice led to Paneth cell and granule abnormalities similar to those observed in Atg16L1^{HM} mice (Fig. 2i and Supplementary Fig. 8), while other epithelial cells appeared normal. This indicates that, within the intestinal epithelium, Paneth cells have a unique sensitivity to autophagy gene disruption.

To better characterize the effects of Atg16L1 deficiency in Paneth cells, we used transmission electron microscopy (EM). We observed degenerating mitochondria, loss of granules, and the frequent absence of apical microvilli in Atg16L1^{HM} Paneth cells (Fig. 3ae; Supplementary Fig. 6d, e). EM also showed Atg16L1^{HM} Paneth cells with marked increases in cytoplasmic vesicles (Fig 3b, d); a similar abnormality has been reported in Paneth cells from a CD patient²⁰. Importantly, such dramatic findings were not present in epithelial progenitors or enterocytes (Fig. 3b, d and Supplementary Fig. 9), confirming that Atg16L1 deficiency selectively affects

Paneth cells within the intestinal epithelium. We next performed transcriptional profiling of Paneth cell RNA procured by laser capture microdissection (LCM)²¹ (see methods and analysis in Supplementary Figure 10). Consistent with a lack of cell death or degeneration as detected by EM, microarray analysis revealed that less than 1.5% of probe sets detected changes in RNA levels using low stringency criteria (≥ 1.3 -fold difference; Supplementary Table 1 and Supplementary Fig. 11). Cluster analysis of significantly enriched transcripts in Atg16L1 deficient Paneth cells revealed a striking signature of genes involved in PPAR pathways, adipocytokine signaling, and aspects of lipid metabolism (Fig. 3f and Supplementary Fig. 12). Additionally, transcripts for several acute phase reactants including serum amyloid A1, haptoglobin, and complement factors D and I were elevated (Fig. 3g). Of particular interest was the observation that the adipocytokines leptin and adiponectin, previously reported to be increased in CD patients^{5,4}, were amongst the most highly enriched transcripts (Fig. 3g). To determine if these transcriptional changes are unique to Atg16L1 deficient Paneth cells, we examined a second primary cell type from Atg16L1^{HM} mice. Autophagy is important in the function of T cells²². Thymocytes from Atg16L1^{HM} mice were normal in number but expressed low levels of Atg16L1 and exhibited decreased conversion of LC3I to LC3II (Supplementary Fig. 13) demonstrating that Atg16L1 is important for autophagy in thymocytes. Microarray analysis of these cells revealed that, in striking contrast to Paneth cells, expression of only 27 genes was altered more than 1.3 fold (Supplementary Fig. 14). There was no significant change in expression of the most significant clusters of transcripts altered in Atg16L1^{HM} Paneth cells, and only one gene altered in thymocytes was also altered in Paneth cells (Fig. 3g). Therefore the transcriptional signature of Atg16L1 deficiency is specific to Paneth cells, again emphasizing the unique effects of Atg16L1 deficiency on these cells. Taken together with the extensive morphologic abnormalities documented above, we conclude that Atg16L1 deficiency is associated with profound alterations in the specialized properties of Paneth cells including defective granule exocytosis and unexpected increases in expression of genes involved in regulating injury responses.

Given the importance of Atg16L1 and Atg5 in Paneth cells in mice, we examined the role of the human *ATG16L1* CD risk allele via a retrospective analysis of ileocolic resection specimens from patients with CD. We studied tissue sections from the uninvolved proximal margins, containing little or no inflammation, from 10 CD patients homozygous for the *ATG16L1* risk allele compared to 7 CD controls without the risk allele. All 17 patients lacked the three major *NOD2* risk alleles and the protective IL23R allele for CD^{7,23}. Independent blinded examination by T.S.S. and E.M.B. revealed that 100% of at risk patients and 0% of controls contained abnormal Paneth cells similar to those in Atg16L1^{HM} mice (Fig. 4a, b). We quantified lysozyme staining in CD patient specimens, and like Atg16L1^{HM} mice, found that patients carrying the *ATG16L1* risk allele contained an increased proportion of Paneth cells with disorganized or diminished granules or exhibiting diffuse cytoplasmic lysozyme staining (Fig. 4c-g). Moreover, consistent with transcriptional analysis in mice, 19% of Paneth cells from at risk patients that exhibited diffuse lysozyme staining also stained positive for leptin protein compared to only 2% of controls ($p < 0.05$) (Fig. 4e, f). These findings demonstrate a remarkable concordance between the pathology and transcriptional profile of Paneth cells from Atg16L1^{HM} mice and Paneth cell abnormalities observed in CD patients with the risk allele of *ATG16L1*. These data provide the first indication that Atg16L1 has a specific role in humans and mice in regulating the specialized properties of Paneth cells, and provide a novel and relevant mouse model that emulates one of the many diverse pathological hallmarks of human CD. We show that Atg16L1 and a second autophagy protein Atg5 are critically important for the known role of Paneth cells in secretion of granule contents that may alter the intestinal microbiota. In addition, we demonstrate a previously unknown role of Atg16L1 in the regulation of Paneth cell expression of adipocytokines previously associated with CD. Within the intestinal epithelium, the dramatic effect of autophagy protein deficiency on Paneth cells, but not enterocytes which share a common progenitor, indicates that autophagy can contribute

to disease pathogenesis via a highly specific role within a single cell lineage. Indeed, the effects of hypomorphic expression of Atg16L1 were specific to Paneth cells and not seen in Atg16L1-deficient thymocytes. An important implication of this type of ‘within-lineage’ specificity is that future studies will need to focus on how Atg16L1 polymorphisms affect the function of differentiated Paneth cells. Since both environment and genotype play a role in human CD pathogenesis⁷, it will be interesting to determine whether environmental triggers including agents that damage the intestine or pathogens alter the pathological features associated with compromised Atg16L1 function.

Supplementary Material

Refer to Web version on PubMed Central for supplementary material.

Acknowledgements

We would like to thank Namiko Abe for technical assistance with fluorescence microscopy, Valleria Cavalli for microscope use, Jason Eisenberg and Aylwin Ng for help with bioinformatics analysis, Andre J. Ouellette for technical advice, and Indira Mysorekar and Jason Mills for help with antibodies. This research was supported by grant U54 AI057160 Project 6 and the Broad Institute (K.C., J.Loh, and H.W.V.), training grant NIH T32 AR07279 (K.C.), the Lallage Feazel Wall Fellowship DRG-1972-08 (K.C.) from the Damon Runyon Cancer Research Foundation; the Pew Foundation (J.Liu., S.L.B., H.M., W.K.C., and T.S.S.); the Washington University Digestive Diseases Research Core Center P30 DK52574, Barnes Jewish Foundation, Johnson and Johnson Translational Seed Award, and the Crohn's Colitis Foundation of America (E.L., S.H., and C.S.); Grants-in-aid for Scientific Research from the Ministry of Education, Culture, Sports, Science and Technology of Japan, and the Toray Science Foundation (C.K. and N.M.); NIH R01 AI062832 (J.A.C.); NIH AI062773 and DK43351 (R.J.X.).

References

1. Barrett JC, et al. Genome-wide association defines more than 30 distinct susceptibility loci for Crohn's disease. *Nat. Genet* 2008;40:955–962. [PubMed: 18587394]
2. Mizushima N, et al. Mouse Apg16L, a novel WD-repeat protein, targets to the autophagic isolation membrane with the Apg12-Apg5 conjugate. *J. Cell Sci* 2003;116:1679–1688. [PubMed: 12665549]
3. Ouellette AJ. Paneth cell alpha-defensin synthesis and function. *Curr. Top. Microbiol. Immunol* 2006;306:1–25. [PubMed: 16909916]
4. Barbier M, et al. Overexpression of leptin mRNA in mesenteric adipose tissue in inflammatory bowel diseases. *Gastroenterol. Clin. Biol* 2003;27:987–991. [PubMed: 14732844]
5. Yamamoto K, et al. Production of adiponectin, an anti-inflammatory protein, in mesenteric adipose tissue in Crohn's disease. *Gut* 2005;54:789–796. [PubMed: 15888786]
6. Genome-wide association study of 14,000 cases of seven common diseases and 3,000 shared controls. *Nature* 2007;447:661–678. [PubMed: 17554300]
7. Xavier RJ, Podolsky DK. Unravelling the pathogenesis of inflammatory bowel disease. *Nature* 2007;448:427–434. [PubMed: 17653185]
8. Rioux JD, et al. Genome-wide association study identifies new susceptibility loci for Crohn disease and implicates autophagy in disease pathogenesis. *Nat. Genet* 2007;39:596–604. [PubMed: 17435756]
9. Hampe J, et al. A genome-wide association scan of nonsynonymous SNPs identifies a susceptibility variant for Crohn disease in ATG16L1. *Nat. Genet* 2007;39:207–211. [PubMed: 17200669]
10. Levine B, Kroemer G. Autophagy in the Pathogenesis of Disease. *Cell* 2008;132:27–42. [PubMed: 18191218]
11. Fujita N, Itoh T, Fukuda M, Noda T, Yoshimori T. The Atg16L Complex Specifies the Site of LC3 Lipidation for Membrane Biogenesis in Autophagy. *Mol. Biol. Cell*. 2008
12. Kuma A, Mizushima N, Ishihara N, Ohsumi Y. Formation of the approximately 350-kDa Apg12-Apg5-Apg16 multimeric complex, mediated by Apg16 oligomerization, is essential for autophagy in yeast. *J. Biol. Chem* 2002;277:18619–18625. [PubMed: 11897782]
13. Stryke D, et al. BayGenomics: a resource of insertional mutations in mouse embryonic stem cells. *Nucleic Acids Res* 2003;31:278–281. [PubMed: 12520002]

14. Kuma A, et al. The role of autophagy during the early neonatal starvation period. *Nature* 2004;432:1032–1036. [PubMed: 15525940]
15. Komatsu M, et al. Homeostatic levels of p62 control cytoplasmic inclusion body formation in autophagy-deficient mice. *Cell* 2007;131:1149–1163. [PubMed: 18083104]
16. Hara T, et al. Suppression of basal autophagy in neural cells causes neurodegenerative disease in mice. *Nature* 2006;441:885–889. [PubMed: 16625204]
17. Madison BB, et al. Cis elements of the villin gene control expression in restricted domains of the vertical (crypt) and horizontal (duodenum, cecum) axes of the intestine. *J. Biol. Chem* 2002;277:33275–33283. [PubMed: 12065599]
18. Porter EM, Bevins CL, Ghosh D, Ganz T. The multifaceted Paneth cell. *Cell Mol. Life Sci* 2002;59:156–170. [PubMed: 11846026]
19. Kobayashi KS, et al. Nod2-dependent regulation of innate and adaptive immunity in the intestinal tract. *Science* 2005;307:731–734. [PubMed: 15692051]
20. Dvorak AM, Dickersin GR. Crohn's Disease: Transmission Electron Microscopic Studies I. Barrier Function. Possible Changes Related to Alterations of Cell Coat, Mucous Coat, Epithelial Cells, and Paneth Cells. *Human Pathology* 1980;11:561–571. [PubMed: 7429506]
21. Stappenbeck TS, Mills JC, Gordon JI. Molecular features of adult mouse small intestinal epithelial progenitors. *Proc Natl Acad Sci U. S. A* 2003;100:1004–1009. [PubMed: 12552106]
22. Pua HH, Dzhagalov I, Chuck M, Mizushima N, He YW. A critical role for the autophagy gene Atg5 in T cell survival and proliferation. *J. Exp. Med* 2007;204:25–31. [PubMed: 17190837]
23. Duerr RH, et al. A genome-wide association study identifies IL23R as an inflammatory bowel disease gene. *Science* 2006;314:1461–1463. [PubMed: 17068223]
24. Subramanian A, et al. Gene set enrichment analysis: a knowledge-based approach for interpreting genome-wide expression profiles. *Proc Natl Acad Sci U. S. A* 2005;102:15545–15550. [PubMed: 16199517]

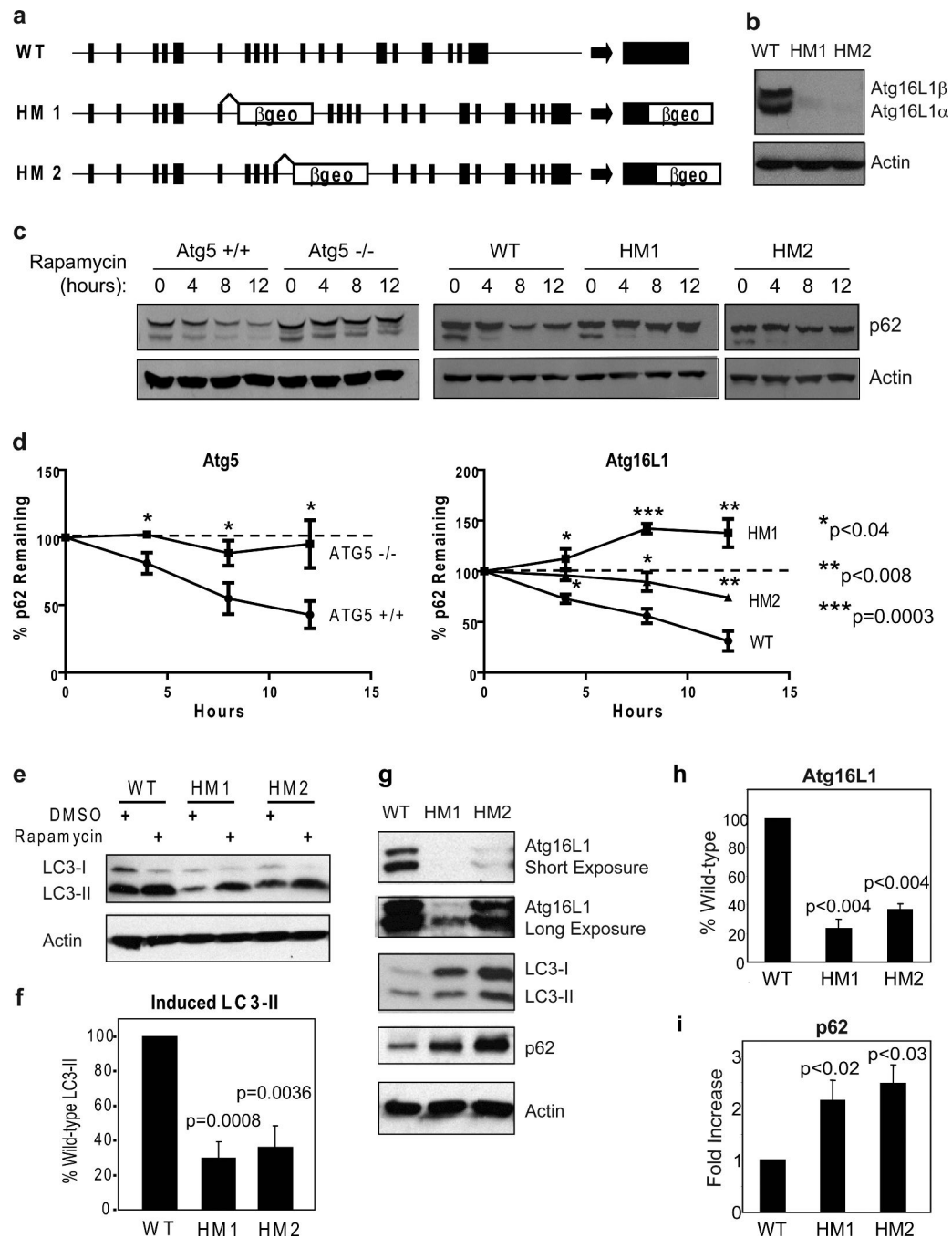


Figure 1. Role of Atg16L1 in autophagy in cells and intestine

a, Gene trap vector containing a splice acceptor followed by the β geo exon disrupts the *Atg16L1* gene locus by insertions within the intronic regions following exon 6 and 10 for the *Atg16L1*^{HM1} and *Atg16L1*^{HM2} lines respectively. **b**, Detection of the α and β isoforms of Atg16L1 by Western blot analysis in whole cell lysates from Murine embryo fibroblasts (MEFs). **c-d**, *Atg5*^{-/-} and *Atg16L1*^{HM} MEFs were grown in the presence of rapamycin (50 μ g/ml) and cyclohexamide (5 μ g/ml) and analyzed by Western blot for loss of p62 expression (**c**) and quantified (**d**) ($n = 3$). **e-f**, Western blot analysis of LC3 expression in MEFs grown in the presence of rapamycin (50 μ g/ml) or DMSO control for 4 h (**e**). Quantification of LC3-II expression in the presence of rapamycin ($n = 6$) (**f**). **g**, Detection of Atg16L1, LC3, and

p62 by Western blot of ileal lysates from Atg16L1^{HM} mice. Atg16L1 can be detected in both mutant lines upon longer exposures. **h-i**, Quantification of Atg16L1 (**h**) and p62 in ileal lysates ($n = 3$). Protein levels were quantified by densitometry and normalized to actin. *P* values were calculated using two-tailed student's *t* test. Error bars represent SEM.

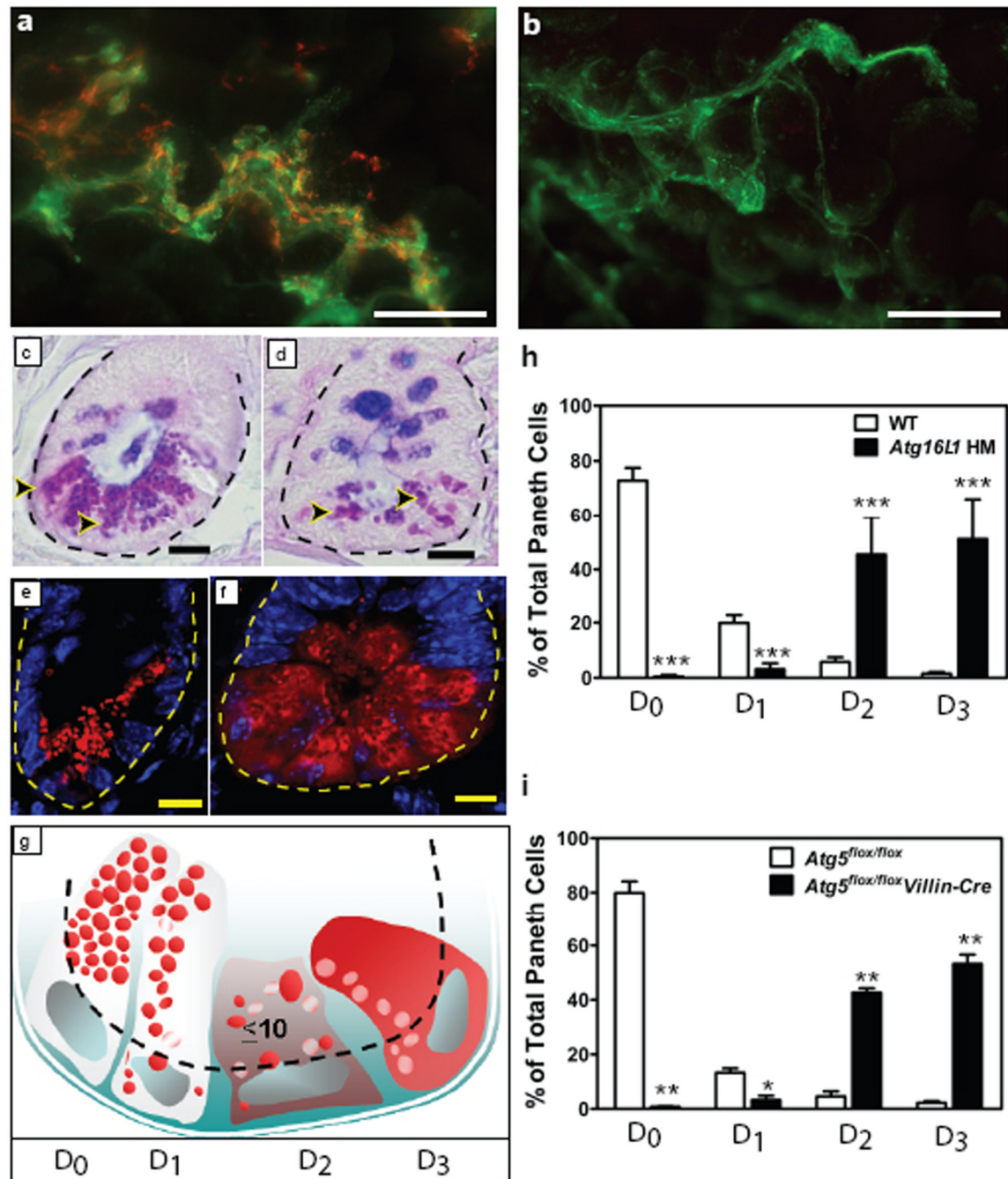


Figure 2. Mutation of Atg16L1 or Atg5 leads to disruption of the Paneth cell granule exocytosis pathway

a-b, Whole-mount images taken immediately above the ileal mucosal surface from WT (**a**) and Atg16L1^{HM} (**b**) mice stained with *Helix pomatia* lectin that labels mucus (green) and antisera directed against lysozyme (red). Images are representative of 3 WT and 3 Atg16L1^{HM} mice. **c-d**, Ileal sections from WT (**c**) and Atg16L1^{HM} (**d**) mice stained with PAS-alcian blue (dotted line denotes crypt unit and arrowheads indicate Paneth cells). Images are representative of 16 WT, 16 Atg16L1^{HM1}, and 14 Atg16L1^{HM2}, greater than 100 crypts analyzed for each. **e-f**, Representative images of indirect immunofluorescence of sections stained for lysozyme (red) in WT (**e**) and Atg16L1^{HM} (**f**) mouse ileal crypts. **g**, Paneth cells

display one of four patterns of lysozyme expression (represented in red, white represents areas that exclude lysozyme): normal (D_0), disordered (D_1), depleted (D_2), and diffuse (D_3). **h-i**, Number of Paneth cells from $Atg16L1^{HM}$ (**h**) and $Atg5^{flox/flox}villin-Cre$ (**i**) mice displaying each pattern of lysozyme expression ($n = 6660$ cells from 5 $Atg16L1^{HM}$ mice and 5634 cells from 5 WT mice; $n = 1756$ cells from 2 $Atg5^{flox/flox}villin-Cre$ mice and 1649 from 2 $Atg5^{flox/flox}$ mice). Scale bars: **a-b**, 200 μm ; **c-f**, 10 μm . * $p < 0.05$, ** $p < 0.01$, *** $p < 0.001$. P values were calculated using two-tailed student's t test. Error bars represent SEM.

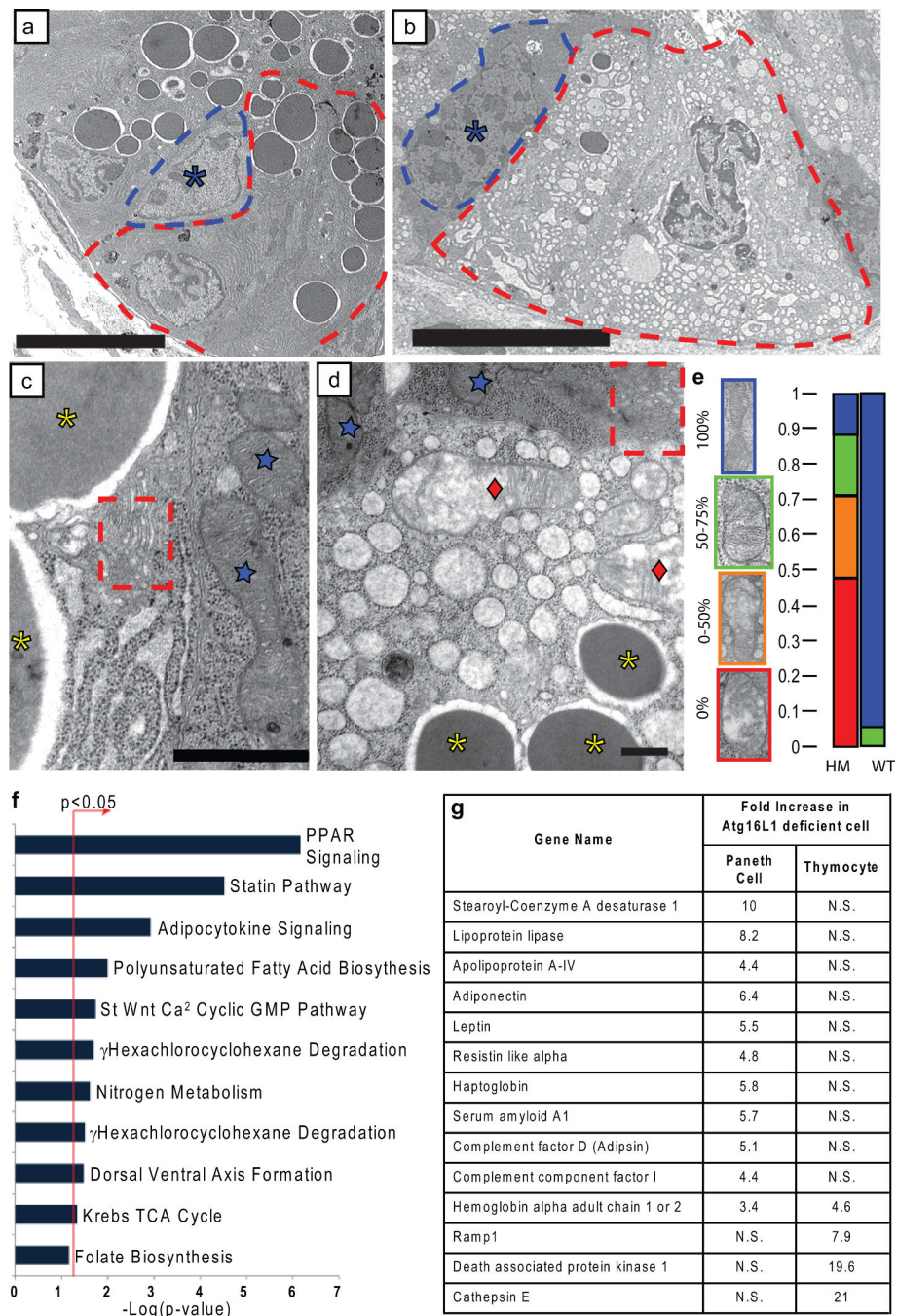


Figure 3. Critical role of Atg16L1 in the structure and transcriptional profile of Paneth cells
a-d, EM of littermate WT (**a**, **c**) and Atg16L1^{HM} (**b**, **d**) Paneth cells (**a**, **b**: dotted lines denote individual cells, asterisk indicates normal progenitor cell; **c**, **d**: blue stars indicate normal mitochondria in WT Paneth cells and Atg16L1^{HM} progenitor cells, red diamonds indicate degenerating mitochondria, dotted Box shows normal Golgi compartments, and yellow asterisks indicate granules) ($n = 3$ mice/genotype). **e**, Mitochondrial integrity was quantified based on the percentage of the visible mitochondrial section displaying intact cisternae ($n = 49$ WT and 71 Atg16L1^{HM} cells). **f**, Enrichment of pathways associated with human orthologs mapped from genes differentially expressed in Atg16L1 deficient Paneth cells relative to WT cells, using the canonical pathway collection from MSigDB²⁴. The bar chart displays the

negative log of the enrichment p-values for each pathway using the hypergeometric distribution (see methods). *denotes pathways found to be significantly enriched ($p < 0.05$). Pathways with only one gene assigned were excluded from the chart. **g**, Chart of selected genes whose mRNA are enriched in either Atg16L1 deficient Paneth cells (baseline = WT Paneth cells) or Atg16L1 deficient thymocytes (baseline = WT thymocytes). N.S. = not significant. Scale bars: **a-b**, 10 μm ; **c-d**, 500nm.

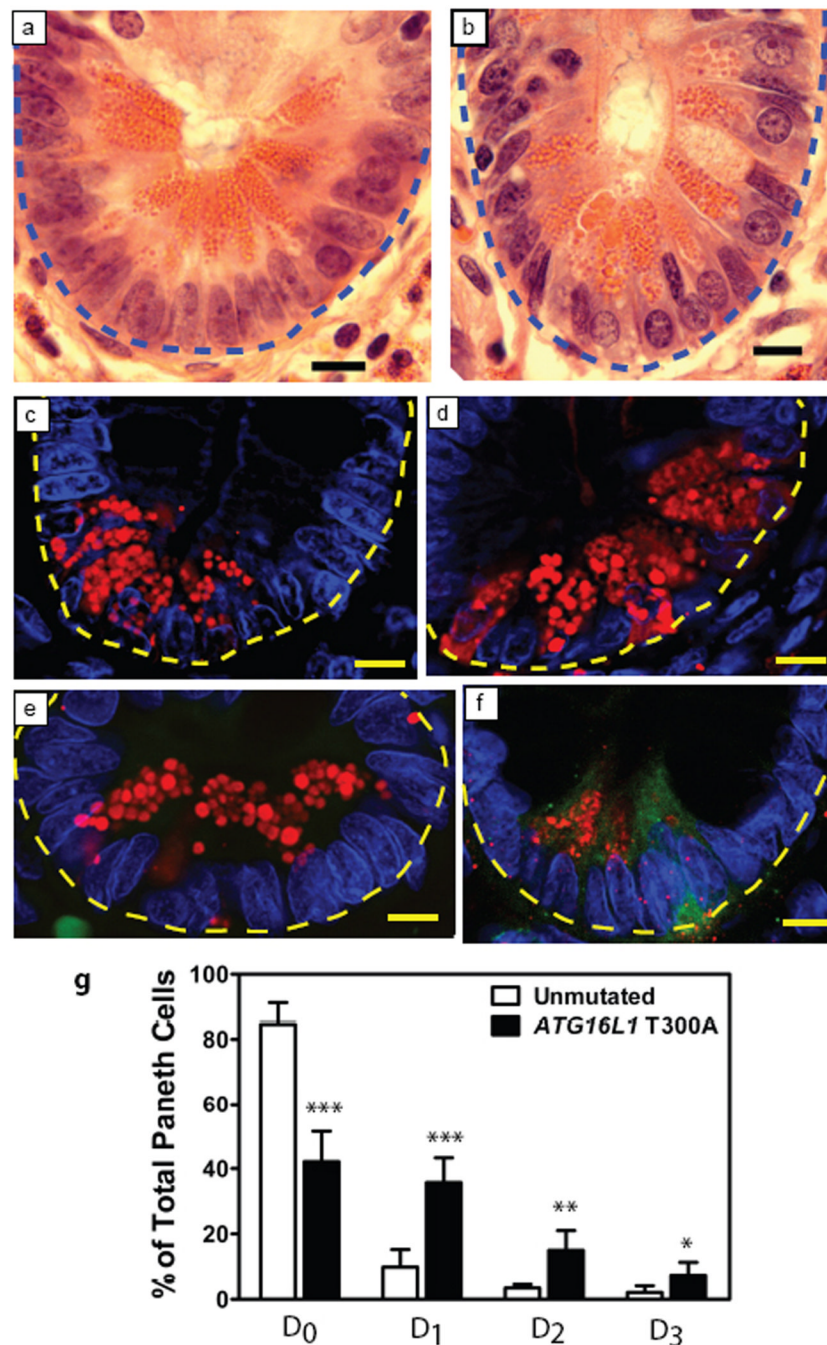


Figure 4. Crohn's Disease patients homozygous for the disease risk allele of *ATG16L1* display Paneth cell abnormalities similar to *Atg16L1*^{HM} mice

a-b, H&E stained sections of uninvolved areas from ileo-colic resections from patients with Crohn's disease homozygous for the safe (**a**) or risk allele (**b**) of *ATG16L1* (blue dotted line denotes crypt unit). **c-f**, Immunofluorescence images of Paneth cells from control (**c**, **e**) and patients with the risk allele (**d**, **f**) stained for lysozyme (red) (**c**, **d**) and double labeled additionally for leptin (green) (**e**, **f**) (yellow dotted line denotes crypt unit). **g**, Aberrant lysozyme expression was quantified by the same criteria used for mouse sections in Fig. 3 (n = 6829 cells for at risk patients and 8182 for control in c and e, n = 5 patients for both genotypes in d and e). Leptin positive D3 cells were quantified in patient samples homozygous for the

risk allele (76/322 D3 cells were positive from a total of 580 crypts examined) and homozygous for the safe allele (11/93 D3 cells were positive from a total 749 crypts examined). Scale bars: **a-f**, 10 μm . * $p < 0.05$, ** $p < 0.01$, *** $p < 0.001$. *P* values were calculated using two-tailed student's *t* test. Error bars represent SEM.